How to cite: *Angew. Chem. Int. Ed.* **2021**, *60*, 8450–8454
International Edition: doi.org/10.1002/anie.202015650
German Edition: doi.org/10.1002/ange.202015650

Fluorescence Probes

Probing the Intracellular Dynamics of Nitric Oxide and Hydrogen Sulfide Using an Activatable NIR II Fluorescence Reporter

Tianli Zhu[+], Ning Ren[+], Xia Liu, Yan Dong, Rongchen Wang, Jinzhu Gao, Jie Sun, Ying Zhu, Lihua Wang, Chunhai Fan, He Tian, Jiang Li, and Chunchang Zhao**

Abstract: *Understanding the complex interplay among gasotransmitters is of great significance but remains technically challenging. In this study, we present the design and synthesis of a dually responsive BOD-NH-SC reporter for probing the dynamic and alternating existence of NO and H_2S in living cells. This designed reporter can repeatedly cycle S-nitrosation and transnitrosation reactions when successively treated with NO and H_2S, thus affording the interchange of NIR fluorescence at 645 nm (NO) and NIR II fluorescence at 936 nm (H_2S). In light of this unique fluorescence alternation between two colors, we synthesized water-soluble BOD-NH-SC dots to visualize the intracellular dynamics of NO and H_2S. These molecular probes thus provide a toolbox to elucidate the interplaying roles of NO and H_2S in the complex interaction networks of various signal transduction pathways.*

Nitric oxide (NO) and hydrogen sulfide (H_2S) are the predominant members of gasotransmitters in mammals, contributing to the regulatory roles in the cardiovascular, nervous, and immune systems.[1] While NO is endogenously synthesized by nitric oxide synthases through the oxidation of L-arginine, H_2S is generated enzymatically from L-cysteine and homocysteine by the action of cystathionine-γ-lyase, cystathionine-β-synthase, and 3-mercaptopyruvate sulfurtransferase.[2] The crucial role of NO and H_2S in many biological processes have individually been identified. Current literatures have also established the importance of the bidirectional relationship between NO and H_2S for modulation of many physiological and pathological processes in living organisms.[3] However, understanding about the correlation between these two gasotransmitters remains woefully incomplete.

Fluorescence imaging, a noninvasive imaging technique with operational simplicity and high spatiotemporal resolution, provides a powerful tool for biomedical and clinical applications.[4] In this context, molecular imaging with H_2S-responsive fluorescent probes has been developed and found widespread applications.[5] Meanwhile, various fluorescent probes that are capable of NO imaging have been developed over the years.[6] Despite these great advantages, evaluating the correlation between NO and H_2S remains an immense challenge. Since HNO is a reactive intermediate generated by the interaction between NO and H_2S, several HNO-responsive fluorescent probes were recently explored for visualizing the NO/H_2S cross-talk in biological systems.[7] However, the specificity and accuracy may be depressed by such indirection assays because HNO do not adequately mimic the complex interplay between NO and H_2S.[8] A simple method, conjugating H_2S-responsive and NO-sensitive fluorophores in a single molecular probe, has been employed to simultaneously measure H_2S and NO.[9] Such designed probe can respond to H_2S, NO, and H_2S/NO with distinct fluorescence signal outputs of green, red and red, respectively. Although the discrimination between NO red and H_2S/NO red signals is realized by independent excitation, high fluorescence background is inevitably introduced due to their high dependence on Förster resonance energy transfer efficiency. Moreover, such probe is incapable of monitoring the dynamic and alternating existence of NO and H_2S in the signal transduction cycles.

To accurately and specifically reporting the interplay between NO and H_2S, we herein report a dual-stimuli responsive BOD-NH-SC with activatable NIR II fluorescence for reporting the dynamic and alternating existence of NO and H_2S. As shown in Figure 1, our molecule features an N-Methyl-2-methoxyaniline moiety as the NO-responsive site. In contrast, the response to H_2S relies on H_2S-initated nucleophilic substitution of 4-nitrobenzenethiol-substituted boron dipyrromethene (BODIPY).[10] In light of the rapid production of N-nitroso product (BOD-NO-SC) upon treatment of BOD-NH-SC with NO, bright NIR emission lighting up at 655 nm was observed. Further incubation with H_2S led to the generation of bright NIR II fluorescence at 936 nm due to the formation of sulfhydryl-functionalized BODIPY (BOD-NO-SH), accompanied by the quenching of the

[*] T. Zhu,[+] Y. Dong, R. Wang, J. Gao, J. Sun, Prof. H. Tian, Prof. C. Zhao
Key Laboratory for Advanced Materials, Institute of Fine Chemicals, School of Chemistry and Molecular Engineering, Frontiers Science Center for Materiobiology and Dynamic Chemistry, East China University of Science and Technology
Shanghai 200237 (P. R. China)
E-mail: zhaocchang@ecust.edu.cn

Dr. N. Ren,[+] X. Liu, Prof. Y. Zhu, Dr. L. Wang, Prof. J. Li
Bioimaging Center, Shanghai Synchrotron Radiation Facility, Zhangjiang Laboratory, Shanghai Advanced Research Institute, Division of Physical Biology, CAS Key Laboratory of Interfacial Physics and Technology, Shanghai Institute of Applied Physics, Chinese Academy of Sciences
Shanghai 201210 (China)
E-mail: lijiang@zjlab.org.cn

Prof. C. Fan
School of Chemistry and Chemical Engineering, Frontiers Science Center for Transformative Molecules and National Center for Translational Medicine, Shanghai Jiao Tong University
Shanghai 200240 (China)

[+] These authors contributed equally to this work.

Supporting information and the ORCID identification number(s) for the author(s) of this article can be found under: https://doi.org/10.1002/anie.202015650.

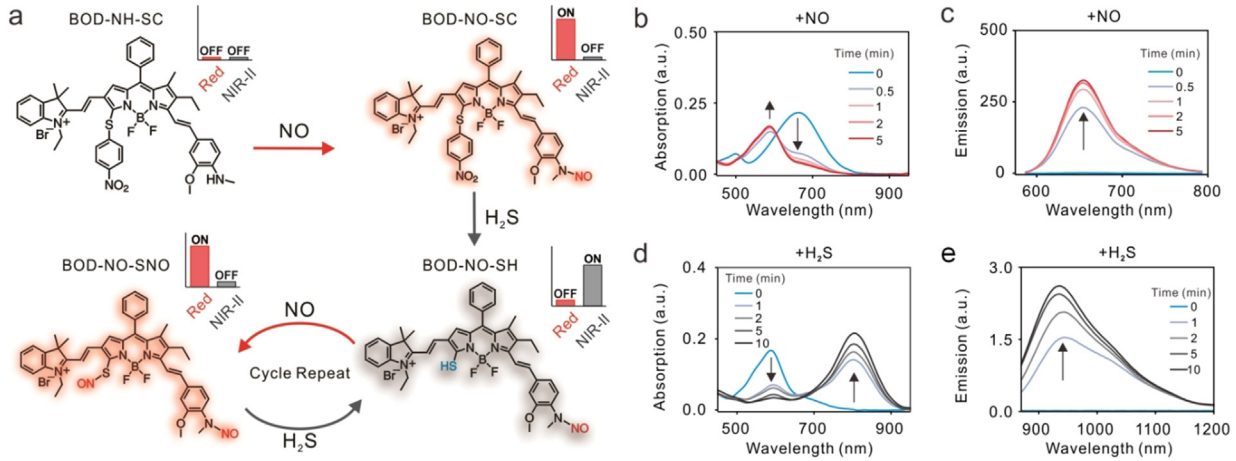

Figure 1. a) Schematic profile of BOD-NH-SC and proposed reaction mechanism with NO and H_2S. Time dependent b) absorption and c) emission changes of BOD-NH-SC (5 μM) in the presence of DEA·NONOate (500 μM). Time dependent d) absorption and e) emission changes of BOD-NO-SC in the presence of H_2S (100 μM).

emission at 655 nm. Notably, the production of sulfhydryl moiety is crucial for reporting the dynamic and alternating existence of NO and H_2S. As demonstrated, treatment of BOD-NO-SH with another portion of NO resulted in the new NIR emission at 645 nm, which can regenerate BOD-NO-SH with emission at 936 nm upon further incubation with H_2S. Specifically, such process is repeatedly cycled, thus capable of accurately monitoring the dynamic and alternating existences of NO and H_2S.

The synthesis of BOD-NH-SC is depicted in Scheme S1. As NO contributes to the production of H_2S in colonic and vascular smooth muscle cells,[3a] we were interested to determine the fluorescence patterns of BOD-NH-SC when successively treated with NO and H_2S. We first verified that BOD-NH-SC showed NO-activatable photophysical features in CH_3CN/PBS buffers (1:1, v/v, 10 mM, pH 7.4, 37 °C). Free BOD-NH-SC displayed a main absorption at 664 nm with minimal fluorescence (Figure 1), which can attribute to an efficient photoinduced electron transfer (PET) from the electron-rich N-Methyl-2-methoxyaniline moiety to the excited BODIPY core. The introduction of DEA·NONOate (500 μM, a commonly employed NO donor) activated a strong absorption at 588 nm, accompanied by a reduction of the original NIR peak at 664 nm (Figure 1b). Such a significant 76 nm hypsochromic shift of the λ_{max} upon treatment with NO could be attributed to the N-nitrosation of N-Methyl-2-methoxyaniline unit to suppress the electron donating strength. Interestingly, the N-nitrosation with NO elicited a fluorescence enhancement of 214-fold at 655 nm under 570 nm light irradiation (Figure 1c). The effective N-nitrosation to produce BOD-NO-SC was confirmed by NMR and HRMS analysis (Figure S1). BOD-NH-SC showed dose-dependent fluorescence responsiveness to NO with a responsive limit of 31 nM (Figure S2). In particular, there was no obvious fluorescence enhancement when BOD-NH-SC was incubated with a variety of reactive species (Figure S3), demonstrating high selectivity of BOD-NH-SC for NO. In addition, good responsiveness was observed between pH 5–9 (Figure S4).

Since a good leaving group 4-nitrobenzenethiol in BOD-NO-SC, H_2S-dependent optical changes could be initiated through aromatic nucleophilic substitution (S_NAr). As expected, the exposure to H_2S led to S_NAr with BOD-NO-SC in test solutions to generate BOD-NO-SH. This transformation was supported by HRMS (Figure S5). In contrast, other reactive sulfur species gave no such S_NAr reaction (Figure S6). Particularly, the S_NAr activated a strong absorption around 806 nm and annihilated the absorption band at 588 nm concomitantly (Figure 1d), affording a distinct red-shift of 218 nm. Importantly, the H_2S-triggered transformation of BOD-NO-SC into BOD-NO-SH elicited a bright NIR-II fluorescence (fluorescence quantum yield of 0.06%) at 936 nm (Figure 1e) with a dose-dependent manner (Figure S7,8), accompanied by quenching of the fluorescence at 655 nm (Figure S9). This lighting up NIR II fluorescence is especially preferable for in vivo bioimaging due to good spatial resolution and highly deep tissue penetration.[11]

In light of the known role of NO action for S-nitrosation,[12] the sulfhydryl moiety in BOD-NO-SH must exhibit rapid reactivity with NO to yield a reactive S-nitrosothiol intermediate (BOD-NO-SNO). Once formed, a transnitrosation reaction[13] between H_2S and BOD-NO-SNO proceeds to release BOD-NO-SH. Such S-nitrosation and transnitrosation processes were repeatedly cycled, which was demonstrated in Figure 2 and Figure S10. Although the NIR II

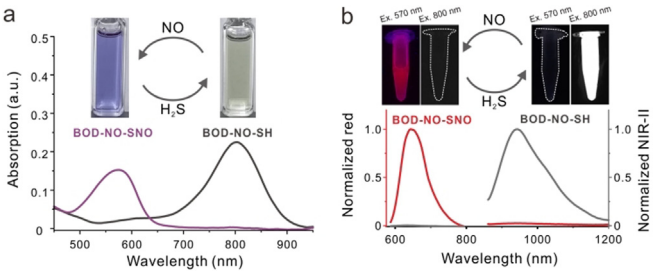

Figure 2. The repeatedly cycled S-nitrosation and transnitrosation processes revealed by optical spectra, a) absorption and b) emission.

fluorescence at 936 nm was attenuated, reaction between BOD-NO-SH and NO afforded a fluorescence turn-on response at 645 nm. The ability of H_2S to participate in transnitrosation reaction led to the regeneration of BOD-NO-SH with NIR II emission at 936 nm. Due to the labile nature of S-nitrosothiols, we employed HRMS analysis of a reductive ligation reaction of BOD-NO-SNO with phenyl 2-(diphenylphosphanyl) benzoate to support the reaction mechanism.[12c] This reductive ligation leads to the sulfenamide 10 and phosphine oxide 11 (Scheme S2). Under our reaction conditions, 10 readily underwent reductive fragmentation to cleave the S−N bond, leading to the formation of 12 and BOD-NO-SH. Notably, BOD-NO-SH showed a significant red-shift in its absorption compared to BOD-NO-SNO due to the NO action for S-nitrosation greatly reduced the electron donating nature, which is consistent with the theoretical calculations (Figure S11). Additionally, the absorption properties of BOD-NO-SH or BOD-NO-SNO remained unchanged in buffer solutions for at last 1 h (Figure S12). However, both BOD-NO-SH and BOD-NO-SNO seemed to undergo complex chemical reaction upon drying, and therefore, no pure BOD-NO-SH and BOD-NO-SNO were obtained for NMR characterizations. Collectively, the repeatedly cycled S-nitrosation and transnitrosation processes by successive treatment with NO and H_2S demonstrated that our probe is a promising tool for accurately monitoring the dynamic and alternating existences of NO and H_2S.

Next, we evaluated the optical changes of BOD-NH-SC when successively treated with H_2S and NO. The presence of H_2S led to an increase in the absorption peak at 840 nm accompanied by a decrease of that at 664 nm (Figure S13). However, relatively weak NIR II emission at 997 nm was triggered with excitation at 840 nm due to the PET from N-Methyl-2-methoxyaniline moiety to BODIPY. This S_NAr reaction proceeded slowly and reached a plateau within 4 hours. At this time point, NO was further introduced to the test solution. The decrease of absorption band at 840 nm along with the emergence of a blue-shifted absorption centered at 581 nm was observed. Upon excitation at 570 nm, gradual enhancement of bright fluorescence around 645 nm was also noted (Figure S14), which was virtually consistent with the transformation of BOD-NH-SH to BOD-NO-SNO. Subsequently, the reversible transnitrosation and S-nitrosation began to cycle when successive addition of H_2S and NO (Figure S15). It should be noted that the slow S_NAr reaction kinetics between BOD-NH-SC and H_2S limited the practical bioimaging applications.

After demonstrating the promising capability of BOD-NH-SC for accurately monitoring the dynamic and alternating existences of NO and H_2S, we then explored the potential for fluorescence mapping in living cells. BOD-NH-SC molecules were first processed into water-soluble and biocompatible BOD-NH-SC dots via direct nanoprecipitation in the assistance of encapsulation matrix 1,2-distearoyl-snglycero-3-phosphoethano -lamine-N-[amino(polyethyleneglycol)-2000] (mPEG-DSPE 2000). The resulting BOD-NH-SC dot was stable in aqueous solution with the hydrodynamic diameter of about 9.8 ± 1 nm as measured by dynamic light scattering (Figure S16). Spherical morphology with an average diameter of around 6 ± 1 nm was also revealed by transmission electron microscopy (TEM) image. The repeatedly reversible responsiveness through S-nitrosation and transnitrosation cycles when successively treated with NO and H_2S was then investigated. It was found that these promising optical responses to NO and H_2S were well maintained within these water-dispersible nanocomposites in PBS buffer solutions (Figure S17). Furthermore, the fluorescence quantum yields of BOD-NH-SC dots in response to NO and NaHS were determined to be 4.56 % (BOD-NO-SC dots), 0.058 % (BOD-NO-SH dots) and 0.04 % (BOD-NH-SH dots) in PBS solutions, respectively.

After identifying the low cytotoxicity of BOD-NH-SC dots toward living cells, we then applied BOD-NH-SC dots to evaluate the alternating presence of NO and H_2S in living colonic smooth muscle and HepG2 cells. As described in Figure 3 and Figure S18, both colonic smooth muscle and HepG2 cells treated with BOD-NH-SC dots gave negligible fluorescence signal in red channel (650–660 nm) and NIR II fluorescence channel (900–1000 nm). However, when the NO-pretreated living colonic smooth muscle or HepG2 cells were loaded with the probe dots, there were bright fluorescence signals in the red channel but minimal fluorescence in NIR II channel. These results suggested that BOD-NH-SC dot was responsive to NO and N-nitrosation of aniline moiety occurred in the living cells. Interestingly, significant fluorescence emergence in NIR II channel concomitant with signal attenuation in red channel were noted when these cells were further treated with NaHS, indicative of H_2S-initiated S_NAr reaction in living cells. Notably, fluorescence enhancement in NIR II channel and attenuation in red channel showed a H_2S dose-dependent manner (Figure S19). Subsequently, successive incubation with another portion of NO and H_2S were performed. As shown in Figure 3 (cycle 2), NO-triggered S-nitrosation in these cells afforded significantly incremental fluorescence in red channel while H_2S-induced transnitrosation led to the generation of bright fluorescence in NIR II channel. These imaging results manifest that BOD-NH-SC is suitable for visualizing the dynamic and alternating existence of NO and H_2S in living cells.

Next, BOD-NH-SC dots were explored for monitoring endogenous H_2S generation with fluvastatin stimulated murine raw 264.7 macrophages in the presence of DEA·NONOate (Figure S20). As observed, the presence of NO in macrophages cells afforded bright red fluorescence but minimal NIR II fluorescence after incubation with BOD-NH-SC dots. Interestingly, a distinct 16.2-fold increase from 0.5 to 8.1 in NIR II fluorescence channel was noted in fluvastatin-stimulated cells when compared with the untreated cells. These imaging experiments indicated that BOD-NH-SC dots could be used for visualization of the existence of endogenous H_2S assisted by NO in living cells.

In summary, we designed and synthesized a dual-stimuli responsive probe BOD-NH-SC for reporting the dynamic and alternating existence of NO and H_2S. This designed probe generated bright NIR II fluorescence when successively treated with NO and H_2S due to the formation of BOD-NO-SH. Of particular importance was that BOD-NO-SH

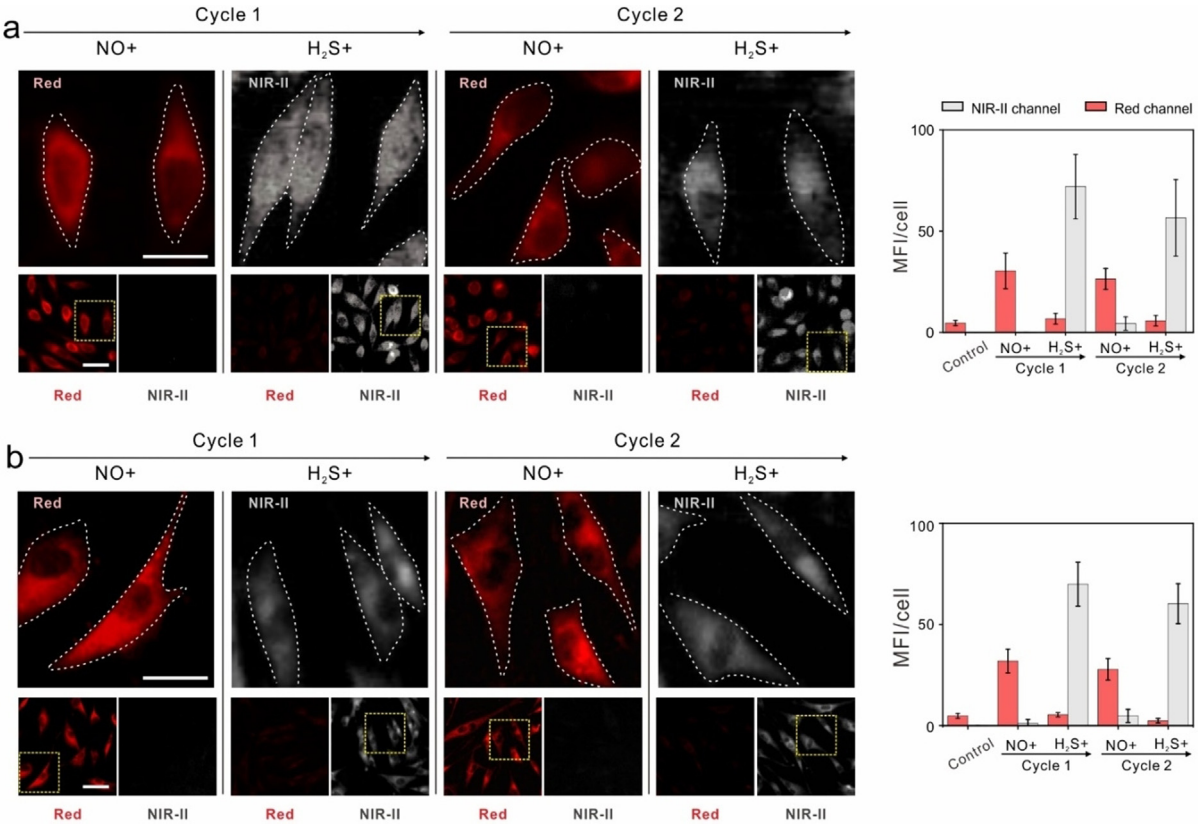

Figure 3. Evaluation of the alternating presence of NO and H_2S in living a) HepG2 and b) colonic smooth muscle cells with BOD-NH-SC dots. Cycle 1 NO+: cells treated with DEA·NONOate (1 mM) for 40 min, followed by incubation with BOD-NH-SC dots for 2 h. Cycle 1 H_2S+: cells of "Cycle 1 NO+" were further treated with NaHS (1 mM) for 2 h. Cycle 2 NO+: cells of "Cycle 1 H_2S+" were further treated with DEA·NONOate (1 mM) for 2 h. Cycle 2 H_2S+: cells of "Cycle 2 NO+" were further treated with NaHS (1 mM) for 2 h. Representative cells (outlined with white dashes in upper rows) are magnified from the boxed regions in the wide-view images (lower rows). Scale bar: 40 μm. Error bars indicate standard deviation from at least three independent tests.

exhibited S-nitrosation reaction in the presence of NO and subsequent H_2S-initiated transnitrosation. Such S-nitrosation and transnitrosation processes were repeatedly cycled, reversibly switching the fluorescence from NIR II at 936 nm to NIR at 645 nm and thus alternating fluorescence between two colors. The formulated BOD-NH-SC dots with good water-solubility and biocompatibility maintained the aforementioned promising optical responses to NO and H_2S, enabling the visualization of the dynamic and alternating existence of NO and H_2S in living cells. This is the first time that monitoring the alternating existence of NO and H_2S with a single fluorescent probe has been realized. We expect that our studies could facilitate the development of unique molecular probes to investigate the complex interplay between NO and H_2S in various signal transduction pathways.

Acknowledgements

We gratefully acknowledge financial support by the National Natural Science Foundation of China (21672062, 21874043, 21788102, 22022410, 82050005, 21834007, 21934007 and 21775157), the Shanghai Municipal Science and Technology Major Project (Grant 2018SHZDZX03), the National Key Research and Development Program (2016YFA0201200), the Shanghai Municipal Science and Technology Commission (19JC1410300) and the Youth Innovation Promotion Association of CAS (Grant No. 2016236).

Conflict of interest

The authors declare no conflict of interest.

Keywords: activatable probe · H_2S · molecular probe · NIR II Fluorescence · NO

[1] a) J. M. Fukuto, S. J. Carrington, D. J. Tantillo, J. G. Harrison, L. J. Ignarro, B. A. Freeman, A. Chen, D. A. Wink, *Chem. Res. Toxicol.* **2012**, *25*, 769–793; b) N. Bashan, J. Kovsan, I. Kachko, H. Ovadia, A. Rudich, *Physiol. Rev.* **2009**, *89*, 27–71; c) G. Yang, L. Wu, B. Jiang, W. Yang, J. Qi, K. Cao, Q. Meng, A. K. Mustafa, W. Mu, S. Zhang, S. H. Snyder, R. Wang, *Science* **2008**, *322*, 587–590; d) D. J. Lefer, *Proc. Natl. Acad. Sci. USA* **2007**, *104*, 17907–17908.

[2] a) C. Nathan, Q.-W. Xie, *Cell* **1994**, *78*, 915–918; b) O. Kabil, R. Banerjee, *J. Biol. Chem.* **2010**, *285*, 21903–21907; c) S. Singh, D. Padovani, R. A. Leslie, T. Chiku, R. Banerjee, *J. Biol. Chem.*

2009, *284*, 22457 – 22466; d) T. Chiku, D. Padovani, W. Zhu, S. Singh, V. Vitvitsky, R. Banerjee, *J. Biol. Chem.* **2009**, *284*, 11601 – 11612.

[3] a) A. D. Nalli, S. Bhattacharya, H. Wang, D. M. Kendig, J. R. Grider, K. S. Murthy, *Am. J. Physiol. Gastrointest. Liver Physiol.* **2017**, *313*, G330 – G341; b) C. Coletta, A. Papapetropoulos, K. Erdelyi, G. Olah, K. Módis, P. Panopoulos, A. Asimakopoulou, D. Gerö, I. Sharina, E. Martin, C. Szabo, *Proc. Natl. Acad. Sci. USA* **2012**, *109*, 9161 – 9166; c) M. Monti, I. Hyseni, A. Pacini, E. Monzani, L. Casella, L. Morbidelli, *Biochem. Pharmacol.* **2018**, *152*, 143 – 152.

[4] a) Y. Yang, Q. Zhao, W. Feng, F. Li, *Chem. Rev.* **2013**, *113*, 192 – 270; b) J. Liang, B. Z. Tang, B. Liu, *Chem. Soc. Rev.* **2015**, *44*, 2798 – 2811; c) F. Wang, Y. Zhu, L. Zhou, L. Pan, Z. Cui, Q. Fei, S. Luo, D. Pan, Q. Huang, R. Wang, C. Zhao, H. Tian, C. Fan, *Angew. Chem. Int. Ed.* **2015**, *54*, 7349 – 7353; *Angew. Chem.* **2015**, *127*, 7457 – 7461; d) H. Zhu, J. Fan, J. Du, X. Peng, *Acc. Chem. Res.* **2016**, *49*, 2115 – 2126; e) L.-Y. Niu, Y.-Z. Chen, H.-R. Zheng, L.-Z. Wu, C.-H. Tung, Q.-Z. Yang, *Chem. Soc. Rev.* **2015**, *44*, 6143 – 6160; f) J. Li, K. Pu, *Chem. Soc. Rev.* **2019**, *48*, 38 – 71.

[5] a) V. S. Lin, W. Chen, M. Xian, C. J. Chang, *Chem. Soc. Rev.* **2015**, *44*, 4596 – 4618; b) M. D. Hartle, M. D. Pluth, *Chem. Soc. Rev.* **2016**, *45*, 6108 – 6117; c) L. Yi, Z. Xi, *Org. Biomol. Chem.* **2017**, *15*, 3828 – 3839; d) C. Zhao, X. Zhang, K. Li, S. Zhu, Z. Guo, L. Zhang, F. Wang, Q. Fei, S. Luo, P. Shi, H. Tian, W.-H. Zhu, *J. Am. Chem. Soc.* **2015**, *137*, 8490 – 8498; e) W. Chen, A. Pacheco, Y. Takano, J. J. Day, K. Hanaoka, M. Xian, *Angew. Chem. Int. Ed.* **2016**, *55*, 9993 – 9996; *Angew. Chem.* **2016**, *128*, 10147 – 10150; f) G. Xu, W. Guo, X. Gu, Z. Wang, R. Wang, T. Zhu, H. Tian, C. Zhao, *CCS Chem.* **2020**, *2*, 527 – 538; g) B. Shi, N. Ren, L. Gu, G. Xu, R. Wang, T. Zhu, Y. Zhu, C. Fan, C. Zhao, H. Tian, *Angew. Chem. Int. Ed.* **2019**, *58*, 16826 – 16830; *Angew. Chem.* **2019**, *131*, 16982 – 16986; h) R. Wang, X. Gu, Q. Li, J. Gao, B. Shi, G. Xu, T. Zhu, H. Tian, C. Zhao, *J. Am. Chem. Soc.* **2020**, *142*, 15084 – 15090; i) L. Wu, Y. Sun, K. Sugimoto, Z. Luo, Y. Ishigaki, K. Pu, T. Suzuki, H.-Y. Chen, D. Ye, *J. Am. Chem. Soc.* **2018**, *140*, 16340 – 16352.

[6] a) L. Teng, G. Song, Y. Liu, X. Han, Z. Li, Y. Wang, S. Huan, X.-B. Zhang, W. Tan, *J. Am. Chem. Soc.* **2019**, *141*, 13572 – 13581; b) Y.-Q. Sun, J. Liu, H. Zhang, Y. Huo, X. Lv, Y. Shi, W. Guo, *J. Am. Chem. Soc.* **2014**, *136*, 12520 – 12523; c) Y. Chen, *Nitric Oxide* **2020**, *98*, 1 – 19; d) C. J. Reinhardt, E. Y. Zhou, M. D. Jorgensen, G. Partipilo, J. Chan, *J. Am. Chem. Soc.* **2018**, *140*, 1011 – 1018.

[7] a) M. Yang, J. Fan, W. Sun, J. Du, S. Long, K. Shao, X. Peng, *Chem. Commun.* **2019**, *55*, 8583 – 8586; b) Y. Zhou, X. Zhang, S. Yang, Y. Li, Z. Qing, J. Zheng, J. Li, R. Yang, *Anal. Chem.* **2017**, *89*, 4587 – 4594.

[8] Q. C. Yong, J. L. Cheong, F. Hua, L. W. Deng, Y. M. Khoo, H. S. Lee, A. Perry, M. Wood, M. Whiteman, J. S. Bian, *Antioxid. Redox Signaling* **2011**, *14*, 2081 – 2091.

[9] a) P. Zhang, J. Li, B. Li, J. Xu, F. Zeng, J. Lv, S. Wu, *Chem. Commun.* **2015**, *51*, 4414 – 4416; b) Y. Zuo, X. Wang, Z. Gou, W. Lin, *Chem. Commun.* **2020**, *56*, 1121 – 1124.

[10] G. Xu, Q. Yan, X. Lv, Y. Zhu, K. Xin, B. Shi, R. Wang, J. Chen, W. Gao, P. Shi, C. Fan, C. Zhao, H. Tian, *Angew. Chem. Int. Ed.* **2018**, *57*, 3626 – 3630; *Angew. Chem.* **2018**, *130*, 3688 – 3692.

[11] a) Q. Yang, Z. Ma, H. Wang, B. Zhou, S. Zhu, Y. Zhong, J. Wang, H. Wan, A. Antaris, R. Ma, X. Zhang, J. Yang, X. Zhang, H. Sun, W. Liu, Y. Liang, H. Dai, *Adv. Mater.* **2017**, *29*, 1605497; b) A. L. Antaris, H. Chen, K. Cheng, Y. Sun, G. Hong, C. Qu, S. Diao, Z. Deng, X. Hu, B. Zhang, X. Zhang, O. K. Yaghi, Z. R. Alamparambil, X. Hong, Z. Cheng, H. Dai, *Nat. Mater.* **2016**, *15*, 235 – 242; c) B. Li, L. Lu, M. Zhao, Z. Lei, F. Zhang, *Angew. Chem. Int. Ed.* **2018**, *57*, 7483 – 7487; *Angew. Chem.* **2018**, *130*, 7605 – 7609; d) Q. Miao, K. Pu, *Adv. Mater.* **2018**, *30*, 1801778; e) C. Li, G. Chen, Y. Zhang, F. Wu, Q. Wang, *J. Am. Chem. Soc.* **2020**, *142*, 14789 – 14804; f) J. Huang, K. Pu, *Angew. Chem. Int. Ed.* **2020**, *59*, 11717 – 11731; *Angew. Chem.* **2020**, *132*, 11813 – 11827.

[12] a) M. W. Foster, D. T. Hess, J. S. Stamler, *Trends Mol. Med.* **2009**, *15*, 391 – 404; b) S. A. Suarez, M. Muñoz, L. Alvarez, M. F. Venâncio, W. R. Rocha, D. E. Bikiel, M. A. Marti, F. Doctorovich, *J. Am. Chem. Soc.* **2017**, *139*, 14483 – 14487; c) H. Wang, M. Xian, *Angew. Chem. Int. Ed.* **2008**, *47*, 6598 – 6601; *Angew. Chem.* **2008**, *120*, 6700 – 6703.

[13] M. R. Filipovic, J. L. Miljkovic, T. Nauser, M. Royzen, K. Klos, T. Shubina, W. H. Koppenol, S. J. Lippard, I. Ivanović-Burmazović, *J. Am. Chem. Soc.* **2012**, *134*, 12016 – 12027.

Manuscript received: November 23, 2020
Revised manuscript received: December 24, 2020
Accepted manuscript online: January 25, 2021
Version of record online: March 3, 2021

